Biogeosciences, 7, 427–440, 2010
www.biogeosciences.net/7/427/2010/

Biogeosciences

A case study of eddy covariance flux of N_2O measured within forest ecosystems: quality control and flux error analysis

I. Mammarella[1], P. Werle[2], M. Pihlatie[1], W. Eugster[3], S. Haapanala[1], R. Kiese[2], T. Markkanen[4], Ü. Rannik[1], and T. Vesala[1]

[1]Department of Physics, University of Helsinki, Finland
[2]Karlsruhe Institute of Technology KIT, Garmisch-Partenkirchen, Germany
[3]ETH Zurich, Switzerland
[4]Finnish Meteorological Institute, Helsinki, Finland

Received: 31 May 2009 – Published in Biogeosciences Discuss.: 14 July 2009
Revised: 31 December 2009 – Accepted: 16 January 2010 – Published: 2 February 2010

Abstract. Eddy covariance (EC) flux measurements of nitrous oxide (N_2O) obtained by using a 3-D sonic anemometer and a tunable diode laser gas analyzer for N_2O were investigated. Two datasets (Sorø, Denmark and Kalevansuo, Finland) from different measurement campaigns including sub-canopy flux measurements of energy and carbon dioxide are discussed with a focus on selected quality control aspects and flux error analysis. Although fast response trace gas analyzers based on spectroscopic techniques are increasingly used in ecosystem research, their suitability for reliable estimates of EC fluxes is still limited, and some assumptions have to be made for filtering and processing data. The N_2O concentration signal was frequently dominated by offset drifts (fringe effect), which can give an artificial extra contribution to the fluxes when the resulting concentration fluctuations are correlated with the fluctuations of the vertical wind velocity. Based on Allan variance analysis of the N_2O signal, we found that a recursive running mean filter with a time constant equal to 50 s was suitable to damp the influence of the periodic drift. Although the net N_2O fluxes over the whole campaign periods were quite small at both sites ($\sim 5\,\mu g\,N\,m^{-2}\,h^{-1}$ for Kalevansuo and $\sim 10\,\mu g\,N\,m^{-2}\,h^{-1}$ for Sorø), the calculated sub-canopy EC fluxes were in good agreement with those estimated by automatic soil chambers. However, EC N_2O flux measurements show larger random uncertainty than the sensible heat fluxes, and classification according to statistical significance of single flux values indicates that downward N_2O fluxes have larger random error.

Correspondence to: I. Mammarella
(ivan.mammarella@helsinki.fi)

1 Introduction

Nitrous oxide (N_2O) is the greenhouse gas with the highest greenhouse warming potential over a long period (100 years). This is about three hundred times larger than that of carbon dioxide (IPCC, 2001). Microbial activity in soil ecosystems is the major source of N_2O to the atmosphere (IPCC, 2001). Agricultural soils are the major sources of N_2O, however, due to their large areal coverage, forest soils have a substantial contribution to the total emissions of N_2O (e.g. Skiba et al., 1994; Kesik et al., 2005).

Due to recent development of fast response N_2O analyzers based on spectroscopic techniques like tunable diode laser (TDL) and more recently quantum cascade laser (QCL) spectrometers, the eddy covariance (EC) method is now suitable for measuring long-term and spatially integrated N_2O fluxes (Neftel et al., 2009).

The EC method is routinely used in many micrometeorological sites worldwide to measure CO_2 and H_2O fluxes above and below forest canopies, thanks to well established methodologies (e.g. Aubinet et al., 2000), based upon long term stability of the fast response CO_2 and water vapour analysers and high signal-to-noise ratios of sampled concentrations. In case of N_2O it is not straightforward that these requirements for reliable estimations of EC fluxes are fulfilled as well. Up to now only a limited number of N_2O EC measurements have been reported in literature and they have been mainly carried out in agricultural soil ecosystems (Smith et al., 1994; Wienhold et al., 1994; Christensen et al., 1996; Laville et al., 1997; Scanlon and Kiely, 2003; Neftel et al., 2007; Kroon et al., 2007), and forest soil ecosystems (Pihlatie et al., 2005; Eugster et al., 2007). Large uncertainty and temporal variability of EC N_2O fluxes, reported by these

studies, are related either to biogeochemical soil processes and/or several systematic and random error sources of the EC measurements. N_2O emissions are episodic in nature, showing high spatial and temporal variability, due to large variation in soil properties such as soil moisture, availability of nitrogen and easily decomposable organic matter (Ambus and Christensen, 1995; Pihlatie et al., 2005; Silver et al., 2005). Emission bursts of short duration, typically occurring after fertilizer application, or associated to thawing and rain events (Flechard et al., 2005, Kroon et al., 2007, Pihlatie et al., 2009), are followed by long periods of small fluxes, when also uptakes of N_2O have been reported (Flechard et al., 2005). Moreover the performance and stability of fast response N_2O gas analyzer strongly depends on the instrumental drift, which typically characterizes TDL and QCL spectrometers (Werle et al., 1993; Nelson et al., 2002). Previous studies performed under field conditions (Eugster et al., 2007; Kroon et al., 2007; Neftel et al., 2009) already noted that the laser drift can cause an over or under-estimation of EC flux. However they did not perform a thorough investigation on the effect of the drift on the calculated flux values. In this case study we explore the limits of eddy covariance flux measurements of N_2O by using state-of-the art equipment. We present a detailed discussion of the main error sources and uncertainties of EC N_2O fluxes measured by a commercially available TDL spectrometer (Campbell Scientific Inc.) within two different forest ecosystems, a beech forest in Sorø, Denmark, and a Scots pine forest in Kalevansuo, Finland, during two distinct measurement campaigns. Both field campaigns were carried out in the trunk space layer. EC system performances are investigated by using the Allan variance concept (Werle et al., 1993). We explored the effect of instrumental drift of the N_2O signal on the EC flux, and we proposed a criterion for selecting a suitable time constant of the high pass filter, which is a necessary method to be applied in order to remove the drift. Flux error analysis, traditionally used in the micrometeorological community for energy and CO_2 fluxes, are discussed and applied to N_2O flux measurements, in order to identify uncertainty of fluxes caused by instrumentation problems and systematic as well as random errors. Finally for validation purposes we compare the EC fluxes with those obtained by soil chamber technique. Recommendations how to treat data for post-processing are derived from the assumption that below-canopy EC flux measurements should match the temporal pattern and magnitude of chamber flux measurements, although also chambers are prone to systematic errors.

2 Site description and measurements

The first measurement campaign was conducted from 2 May to 5 June 2003 in a 87 year old beech (*Fagus sylvatica* L.) forest near Sorø on the island of Zealand, Denmark (55°29′ N, 11°38′ E). The annual precipitation is 650 mm and the mean temperature 8 °C. The forest is located in a flat terrain and extends 1 km in the east-west direction and 2 km in north-south direction. The beech trees are 25 m tall, but the forest also contains scattered stands of conifers. The mean leaf area index (LAI) for the main footprint of the forest is $5\,m^2\,m^{-2}$. The LAI is approximately constant between June and September and drops slowly during the autumn. During the campaign EC N_2O fluxes were measured in the sub-canopy layer at 3 m height above the forest floor by using a small mast. The EC system consisted of a 3-D sonic anemometer (Solent 1012, Gill) and a TDL gas analyser (TGA 100, Campbell Scientific Inc.). Soil N_2O fluxes were also obtained by using chamber technique. More details on the chamber setup and data processing are given in Pihlatie et al. (2005).

The second measurement campaign was conducted during the spring 2007 (25 April to 27 June) at a Kalevansuo drained peatland forest. The site was located in southern Finland (60°39′ N, 24°22′ E), where the mean annual precipitation is 606 mm and the mean annual temperature is 4.3 °C. The canopy height is about 16 m, the tree stand is uneven and unclosed, and consists mainly of Scots pine (*Pinus sylvestris* L.) with some small-sized Norway spruce (*Picea abies* L.) and downy birch (*Betula nana*) in the gaps near ditches. The total LAI is approximately $2\,m^2\,m^{-2}$. EC measurements of CO_2, H_2O and N_2O fluxes were performed at 4 m height above the forest floor. Sub-canopy CO_2 and H_2O fluxes were measured by a Li-7500 Open-Path Infrared CO_2/H_2O Gas Analyzer (Li-Cor Inc.) and a CSAT3 Sonic Anemometer (Campbell Scientific Inc). EC measurements of N_2O fluxes were conducted at the same mast using the same CSAT3 anemometer and a TDL spectrometer (TGA-100A, Campbell Scientific Inc.). Soil fluxes of N_2O were also measured by enclosure method using automatic and manual chambers. The nine automatic chambers sampled and analyzed continuously by gas-chromatography were located approximately 100 m southwest from the sub-canopy EC mast. More details on chamber setup and data processing are given in Pihlatie et al. (2009).

The TDL system used in both sites consists of a temperature and current controlled single mode diode laser, tuned to an infrared N_2O absorption band and mounted in a liquid nitrogen Dewar. Concentration measurement was achieved by passing the infra red laser beam through the sample and reference cells. The reference gas (2000 ppm N_2O from a steel cylinder) was drawn through the reference cell under same temperature and pressure conditions as the sample air in the sample cell (see Table 1 for temperature and pressure values). The sample air was drawn to the TDL analyzer with a Busch rotary-vane pump (RB0021-L) via a diffusive dryer (PD1000, Perma pure Inc.) to remove excess water vapour that could infer the analysis. Sample air leaving the dryer was directed to the TDL analyzer via 10 m long Teflon tubing (inner diameter 4 mm) for Sorø and 4 m for Kalevansuo (inner diameter 4.25 mm). The total volume of the inlet system was

Table 1. The setup details of the two EC-TDL systems.

Site	Kalevansuo	Sorø
Sonic anemometer	CSAT3 – Campbell	Solent 1012 - Gill
N_2O analyser	TGA 100 A – Campbell	TGA 100 – Campbell
CO_2 and H_2O analyser	Li-Cor 7500	–
Inlet height	4 m	3 m
N_2O sampling tube	PE aluminium composite (synflex 1300)	PTFE Teflon
Length	4 m	10 m
Outer/inner diameter	9.75 mm/4.25 mm	6 mm/4 mm
Dryer	142 cm Nafion dryer (PD1000, Perma pure Inc.)	142 cm Nafion dryer (PD1000, Perma pure Inc.)
Sample cell (length)	1.5 m	1.5 m
-volume	480 ml	480 ml
-flow	15 slpm	14 slpm
-pressure	50 mbar	70 mbar
-sampling cell response time (effective bandwidth)	0.095 s (1.67 Hz)	0.14 s (1.12 Hz)
Horizontal spatial separation between sonic probe and N_2O inlet	0.15 m	0.1 m
Pump	Busch rotary-vane pump (RB0021-L)	Busch rotary-vane pump (RB0021-L)
Reference gas	2000 ppm in reference cell (Messer Griesheim, Germany)	2000 ppm in reference cell (Oy Aga Ab, Linde Gas)

approximately 0.24 l and that of the sample cell 0.48 l. The sample flow rate was 14 l min^{-1} for Sorø and 15 l min^{-1} for Kalevansuo experiment. The residence time in the sample cell was approximately 0.1 s, which is sufficient to provide the necessary exchange time for flux measurements.

During the measurement period, pressure inside the sample cells was kept constant at approximately 70 mbar for Sorø and 50 mbar for Kalevansuo and at both sites the measurements were conducted at 10 Hz frequency. The TDL used at Sorø was calibrated once during the measurement campaign using zero and span (290.3 ppb N_2O) calibration gases, while at Kalevansuo the factory calibration was used. The setup details and operational parameters according to the data sheet of the two EC-TDL systems are summarized in Table 1.

3 Methods

3.1 EC measurements: data processing and corrections

The EC fluxes were calculated as 30 min co-variances between the scalars and vertical wind velocity according to commonly accepted procedures (e.g. Aubinet et al, 2000). Prior to calculating the turbulent fluxes a 1-D rotation (mean lateral wind equal to zero) of sonic anemometer wind components and filtering to eliminate spikes were performed according to standard methods (Vickers and Mahrt, 1997).

All signals were detrended for removing the average values and trends. As a first step a linear detrending (LDT) procedure was used. However, the N_2O signal measured by the TDL gas analyzer was frequently dominated by low frequency noise, which is mainly due to optical interference fringes (Campbell TDL Reference Manual; Hernandez, 1986; Werle et al., 2004; Brodeur et al., 2008), and in turn has strong effect on the system performance and the flux detection limit. The movement of the fringes (and thus the change in the N_2O offset) is influenced by the instrument temperature (Smith et al., 1994), and it can contaminate the flux in the case that 1) these offset drift changes are faster compared to the eddy correlation averaging time and 2) the resulting concentration fluctuations are correlated with the vertical wind velocity fluctuations. In order to suppress the instrumental drift and its potential effect on the estimated flux values, the N_2O flux was also calculated after applying an autoregressive running mean filter (RMF, McMillen, 1988) to the sampled signals. Although this approach was adopted previously for post-processing drifting concentration signals (Billesbach et al., 1998; Kormann et al., 2001; Kroon et al., 2007), the choice of the high pass time constant is not straightforward and objective selection methods are rare in literature (Werle, 2009). Methods based on signal auto-correlation coefficient and spectral analysis likely fail to give a reliable estimation of the timescale at which the drift effect becomes important, because of non-stationarity nature

of the low frequency signal noise. In this study we used the concept of the Allan variance (see Appendix A), as proposed by Werle et al. (1993). This technique is a valuable tool to assess the precision and stability of TDL spectrometers and has been used to get an estimate for the time constant for the running mean filter as described in Sect. 4.1.

The lag time between the N_2O signal and vertical wind speed was determined by maximizing the corresponding cross-covariance function, using a procedure similar to Pihlatie et al. (2005). The measured N_2O lag time was about 1 s for Kalevansuo and 2 s for Sorø.

Systematic flux underestimation due to the system characteristics results from physical limitations in the sensor response times, separation distances between the sonic probe and the gas inlet, size of the sensors, the use of sampling line filters, and the sampling tube dimensions. Therefore, these limitations concern only the high frequency band of the scalar fluctuations. All mentioned effects could be described quantitatively by transfer functions according to Moncrieff et al. (1997) and Aubinet et al. (2000) and the flux loss can be estimated by using cospectral correction method (Moore et al., 1986; Horst, 1997, Eugster and Senn, 1995, Mammarella et al., 2009). In this study under the assumption of cospectral similarity between fluxes of CO_2, N_2O and sensible heat, all fluxes were corrected for low-pass filtering effects by using an empirical cospectral model (derived from sensible heat cospectra) and theoretical transfer functions.

Cospectra of sensible heat, CO_2 (only for Kalevansuo) and N_2O were calculated using fast Fourier transform (FFT) on segments of 2^{15} data points (about one hour periods). In order to reduce the random uncertainty, the single cospectra were ensemble averaged according to atmospheric stability.

In order to quantify the high frequency flux loss, a below canopy cospectral model was empirically derived by fitting the sensible heat cospectra $\mathrm{Co}_{w\theta}$, to this simple functional form:

$$\frac{f\mathrm{Co}_{w\theta}}{\overline{w\theta}} = \frac{n}{n_m}\left[1+m\left(\frac{n}{n_m}\right)^{2\mu}\right]^{-\frac{1}{2\mu}\left(\frac{m+1}{m}\right)} \quad (1)$$

where f is the natural frequency in Hz, n= fz/U is the normalized frequency, z the EC measurement level, U the mean wind velocity, m is the inertial slope parameter (which should be equal to 3/4 in order to get the $-4/3$ inertial sub-range power law of the cospectrum $f\mathrm{Co}_{w\theta}$), μ is the broadness parameter and n_m is the normalized frequency at which the logarithmic cospectrum $f\mathrm{Co}_{w\theta}$ attains its maximum value (Lee et al., 2004). The measured sensible heat cospectra were fitted to the Eq. 1 by non-linear regression obtaining the parameters m, μ and n_m The results are discussed in Sect. 4.2.

The correction for density fluctuations (Webb et al., 1980) was not necessary for N_2O flux measurements because moisture has been removed by using a high flow sample dryer in the system (PD1000 Nafion® dryer, Campbell Scientific, Inc., Logan, UT, USA).

3.2 Random error of flux estimates

The time-averaged co-variance $\overline{w'c'}$ is a random variable estimated over a finite realisation and its average departure from the ensemble average $< w'c' >$ is presented by the random error δF, which is a measure of one standard deviation of the random uncertainty of turbulent flux observed over an averaging period T (Lumley and Panofsky, 1964, Lenschow et al., 1994). The random error δF associated with $\overline{w'c'}$ is generally due to stochastic nature of turbulence and instrumental noise.

The random error δF of turbulent flux observed over an averaging period T was evaluated according to Vickers and Mahrt (1997)

$$\delta F = \sigma_F \mathrm{N}^{-1/2} \quad (2)$$

where the period T (30 min) is divided into N=6 sub-records and σ_F= $(< F_i^2 > - < F_i >^2)^{1/2}$ is the standard deviation of the sub-record average fluxes F_i ($i = 1, \ldots \mathrm{N}$), where $<\ >$ denotes averaging over N sub-record values.

4 Results

4.1 TDL system stability and performance

The ability of performing EC flux measurements by using the EC-TDL system depends on the accuracy and stationarity of the N_2O signal measured by the TDL spectrometer. Moreover the system needs to operate continuously under changing environmental conditions in the field. In order to investigate the short term stability of the N_2O gas analyzer, the system was evaluated in the laboratory by sampling a constant source of N_2O from closed laboratory room. The flow system was the same than what was used in the field, resulting in similar sample flow and cell pressure. An Allan variance analysis was performed to the N_2O concentration measurements and the 10 Hz noise level (std) of TDL was estimated to be 1.5 ppbv, which is in line with the system specifications from the manufacturer. A typical drift timescale (defined as the minimum of Allan variance) for the TDL used in this study was also determined in the lab, and it is about 120 s. Nelson et al. (2004) found a Allan variance stability time of about 100 s for N_2O and 200 s for CH_4 for the Aerodyne Research pulsed QCL spectrometer.

The spectrometer stability can be definitely worse under field conditions, where the temperature changes cannot be fully controlled as in a laboratory environment. Moreover additional low frequency drift in the scalar concentration may be due to non-stationarity of the atmospheric signal. During both measurement campaigns, TDL systems were inside a box and the insulated enclosure cover, recommended by the manufacturer, was used in order to dampen diurnal temperature variations. We frequently observed slow variations in the N_2O concentration signal, which cannot be related to

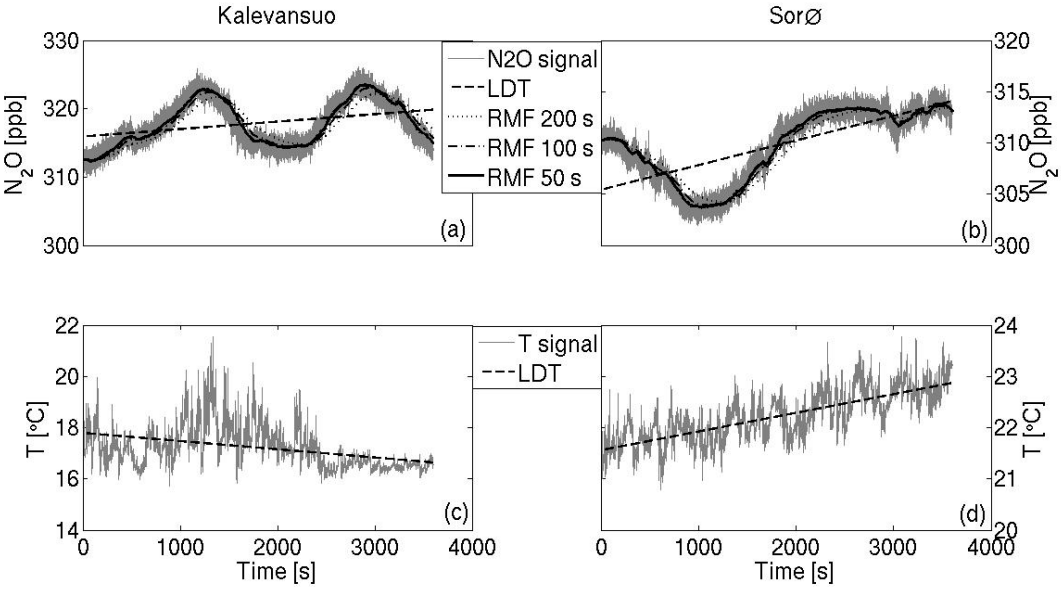

Fig. 1. Example of 1 h time series of N_2O concentration measured at Kalevansuo (18 May 2007, 15–16 h) and Sorø (15 May 2003, 12–13 h), showing the effect of optical interference fringes (**a** and **b**). The sonic temperature signals are also displayed for comparison (**c** and **d**). Dark lines represent linear trend (LDT) and running mean (RMF) with different time constant applied to the data.

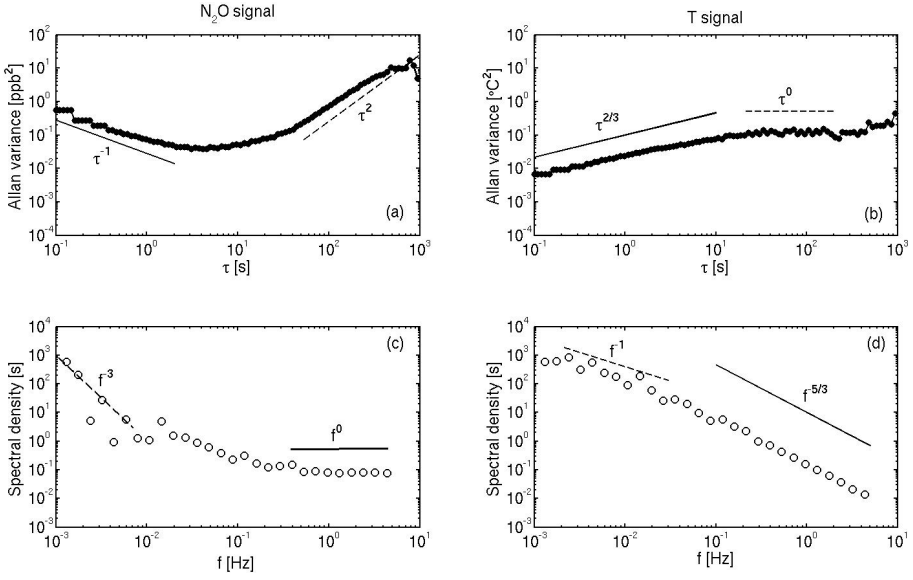

Fig. 2. (a) and **(b)**: Allan variance plot of N_2O and sonic temperature time series displayed in Fig. 1a, c (Kalevansuo site). **(c)** and **(d)**: The corresponding normalized spectral densities. Lines show the slope of different domains characterizing the signals (see the text).

non-steady-state conditions of turbulent motions, since other scalars were not affected, but they are mainly caused by laser drift. An example is given in Fig. 1, where one hour of N_2O and sonic temperature signals, measured at Kalevansuo and Sorø, are displayed. The N_2O concentration signal has a wave-like shape, which is not properly removed when using a LDT operation. For this case we found that a recursive high pass filter with a time constant of about 50 s suppresses the influence of low frequency drift to the N_2O signal. By using larger time constants (100 and 200 s), the running mean tends to lag with respect to the actual trend. Instead, the temperature signal measured at both sites is not affected by the same kind of low frequency noise, and a simple LDT operation was suitable. Figure 2 shows the corresponding Allan variance and FFT spectra of N_2O and T signals measured at Kalevansuo. In the lower part of Fig. 2 we can see that there

Table 2. Fitting parameter values of cospectral model (Eq. 1) applied to sub-canopy sensible heat cospectra measured during daytime at Kalevansuo and Sorø site.

Parameters	m	Inertial sub-range slope (m+1)/m	μ	n_m
Kalevansuo	1.004	2	0.84	0.122
Sorø	1.06	1.94	1.02	0.07

is a correspondence between the slope α of the FFT spectrum and the slope β of the Allan variance, e.g. $\alpha = (-\beta - 1)$. For example, $\alpha = 0$ corresponds with $\beta = -1$ for white noise, and $\alpha = -3$ corresponds with $\beta = 2$ for a linear drift (Werle et al, 1993).

The N_2O Allan variance (Fig. 2a) indicates that the signal is dominated by white noise up to about 5 s and it starts to drift after 50 s. Both regimes are clearly observable in the time domain (Allan variance) as well as in the frequency domain (spectrum), and they are identified by the corresponding slopes α and β. For comparison the temperature does not show any such drift at large timescales (low frequencies), but mainly consists of two domains: an inertial sub-range and a domain showing a slope $\beta = 0$ ($\alpha = -1$), likely related to inactive turbulent eddies (Katul et al., 1998), penetrating down into sub-canopy layer. It seems that the low frequency range of the N_2O signal (< 0.02 Hz) is mainly dominated by instrumental drift, which can give an artificial extra contribution to the fluxes when the resulting concentration fluctuations are correlated with the fluctuations of the vertical wind velocity. For all analysed cases, when the N_2O signal was dominated by a fringe effect, we found that a high-pass filter time constant of 50 s was suitable to damp the influence of the periodic drift.

The same analysis was done with Sorø N_2O time series and similar results were found, as shown in Fig. 3. However, the fringe effect was observed less frequently during the Sorø campaign and mainly during the first half of the measuring period.

4.2 Cospectra

The empirical cospectral model (Eq. 1) was fitted to the sensible heat cospectra, measured at both sites during daytime conditions. The averaged frequency weighted cospectra of the sensible heat flux are shown in Fig. 4a and c for Kalevansuo and Sorø respectively, and the fitting parameter values are displayed in Table 2. Prior to averaging operation, it was established that the fitting parameters were not a function of atmospheric stability under near-neutral or unstable daytime conditions.

In the inertial sub-range the sensible heat flux cospectra $Co_{w\theta}$ measured within the trunk space are less steep than the expected surface layer slope $-7/3(-2.33)$ (Kaimal et al., 1972), and the transfer of energy from the production to the dissipation scales follows a slope equal to about -1.94 for Sorø and -2 for Kalevansuo (Table 2). Similar result was obtained by Amiro (1990) inside three different types of forest canopies (aspen, pine and spruce). The average value of the normalized frequency n_m is smaller for Sorø (0.073) than the one estimated for Kalevansuo (0.12). This difference is likely due to the different height of the canopies (25 vs. 16 m). In the roughness sub-layer the scalar transport is dominated by coherent structures (ejection-sweep cycle), whose typical length scales are proportional to the canopy height h_c (Kaimal and Finnigan, 1994). Hence the difference in n_m between the two sites could be explained just defining a new normalized frequency $n_{mh} = n_m\ h_c/z = f_m\ h_c/U$ (here we should acknowledge that a general scaling for the spectral peak would imply to use the wind velocity measured at the canopy top U_{hc} instead of U, but unfortunately measurements of U_{hc} were not available for these sites). Using the canopy height h_c instead of the measurement height z, the normalized frequency values at which the cospectra peak, occur at 0.6 for both sites, which indicates that the most energetic eddies scale with h_c and that for the selected cases the ratios U_{hc}/U are invariant between the two sites. While such a simple cospectral model described very well the sensible heat cospectra measured during daytime, it was found unsuitable for fitting the night-time measured cospectra, which were often characterized by larger uncertainty as a result of multi-scale non-stationary processes usually affecting the night-time scalar transport in the sub-canopy layer (Cava et al., 2004).

The N_2O cospectra (Fig. 4b and d) show more random variability especially in the low frequency range, where contributions with opposite direction to the total covariance are measured and the effect of N_2O signal drift is clearly evident. Instead at higher frequencies the N_2O cospectra behave similarly to the sensible heat, except that they show a damping effect at the end of the inertial sub-range, as discussed in the following section.

4.3 Flux systematic error

In order to assess the applicability of the cospectral transfer function method in the sub-canopy layer, we simulated first the high frequency loss of CO_2 flux, whose measured cospectra show less random uncertainty than those of N_2O fluxes. At Kalevansuo site the CO_2 flux loss is mainly due to the separation distance between the sonic probe and the head of the Licor 7500. The effective first-order transfer function was also experimentally estimated as a ratio between the measured normalized cospectrum of the CO_2 and sensible heat flux (Mammarella et al., 2009). The normalizing factors were calculated over frequencies not affected by attenuation (Aubinet et al., 2000). Figure 5 shows the predicted and measured CO_2 cospectra calculated during daytime and a typical mean value of sub-canopy wind velocity of 0.7 m s^{-1}.

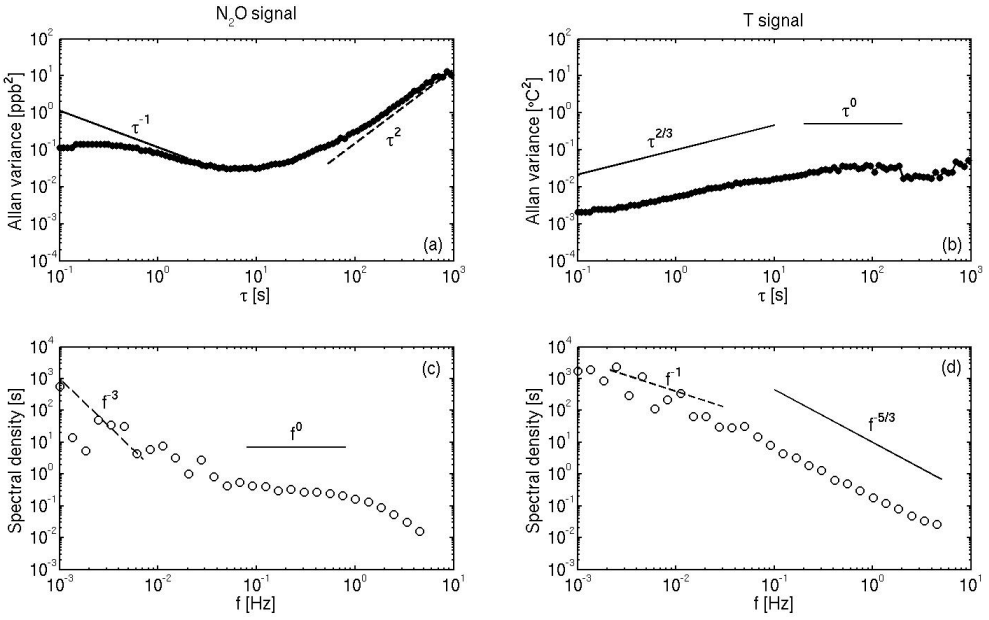

Fig. 3. The same as Fig. 2 for the time series displayed in Fig. 1b, d (Sorø site).

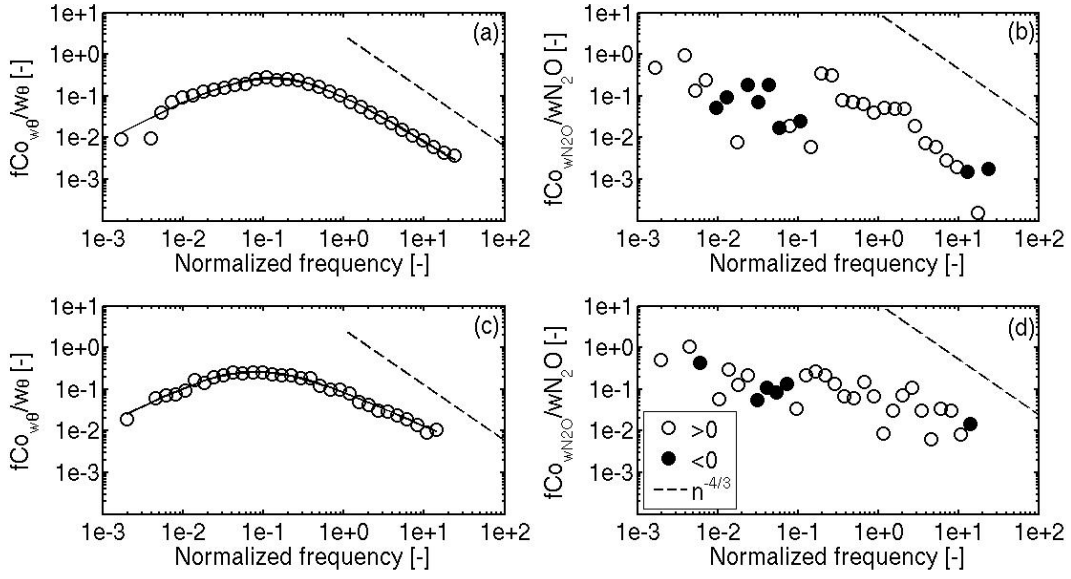

Fig. 4. Ensemble averaged cospectra of sensible heat and N_2O fluxes measured under unstable stratification during the Kalevansuo (**a** and **b**) and Sorø (**c** and **d**) campaigns. The wind velocity was $0.8\,m\,s^{-1}$ and $0.6\,m\,s^{-1}$ for Kalevansuo and Sorø respectively. The solid line is the fitted cospectral model (Eq. 1) and dashed line indicates the theoretical inertial sub-range slope.

Here the predicted cospectra for CO_2 refer to the normalized temperature cospectrum damped either by using the effective transfer function or the theoretical ones according to Moncrieff et al. (1997). In all analysed cases, both methods were suitable for estimating the CO_2 flux loss, which was about 5%. Despite the fact that the within canopy turbulence at small scale likely is not isotropic, the high frequency flux loss during daytime conditions was rather well simulated and predicted by using cospectral correction methods.

In the case of the TDL-EC system, the spatial separation between the sonic probe and the sample gas inlet together with the TDL optical measurement cell response time caused the largest part of the high-frequency underestimation. Although the N_2O cospectra measured at both sites are remarkably noisier than the previously shown CO_2 cospectrum, the damping of the highest frequencies for Kalevansuo is broadly predicted by the sensible heat cospectra attenuated by the appropriate transfer functions (Fig. 6a). For the

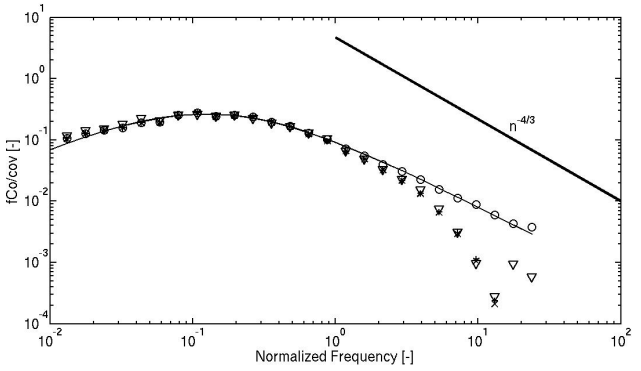

Fig. 5. Example of normalized cospectra of sensible heat (open circle) and carbon dioxide (open down triangle) fluxes measured under unstable stratification during the Kalevansuo campaign. The solid curve is the fitted cospectral model (Eq. 1) and the plus and cross symbols are the predicted CO_2 cospectra computed by multiplying the cospectral model by the theoretical and empirical transfer functions for CO_2 respectively.

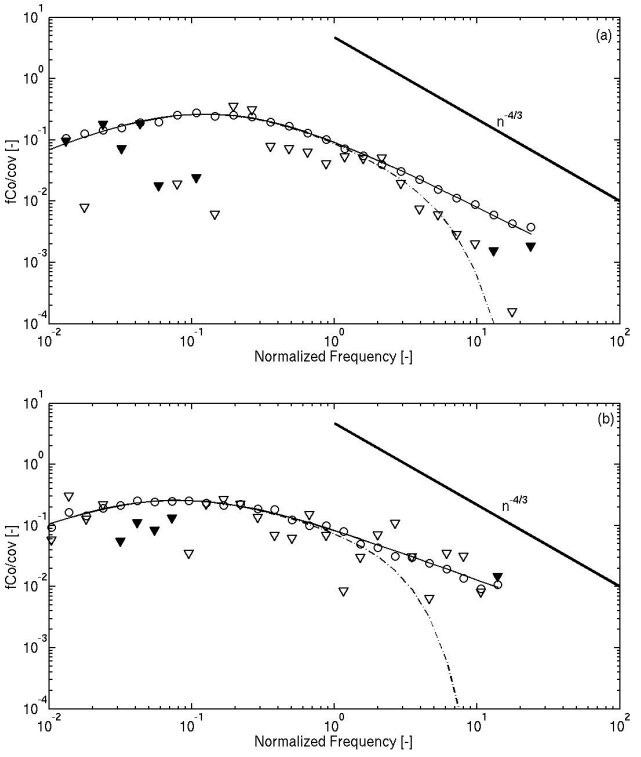

Fig. 6. Example of normalized cospectra of sensible heat (open circle) and N_2O (down triangle) fluxes measured under unstable stratification during the **(a)** Kalevansuo and **(b)** Sorø campaigns. The solid curve is the fitted cospectral model (Eq. 1) and the dash-dotted line is the predicted N_2O cospectra computed by multiplying the cospectral model by the theoretical transfer function for N_2O. The open and closed down triangles refer to positive and negative values respectively.

Sorø site (Fig. 6b) the measured N_2O cospectrum surprisingly does not show similar damping at the high frequency end. Besides the random uncertainty of cospectral density estimates, such behaviour is likely related to the EC digital filter of the TDL system used during the Sorø campaign. In fact the corresponding N_2O spectrum showed an "apparent" $-5/3$ inertial sub-range at the high frequency end (Fig. 3c), where we would expect a signal dominated by white noise. The resulting flux reduction was less than 10% for both sites.

Finally the systematic flux error due to the high pass running mean filter (RMF) should be corrected by using the appropriate transfer function (Rannik and Vesala, 1999) and the fitted empirical cospectral model. However, in practical, we did not include such correction in the final flux values, because a correction would require a priori knowledge about the instrumental interference structure. Moreover cospectral similarity does not necessarily apply at low frequency range. More research should be done on this issue.

4.4 Flux random uncertainty

Random flux error of N_2O and sensible heat flux measurements were estimated according to Eq. 2 for Kalevansuo and Sorø datasets. Figure 7 (top panels) shows the frequency distributions of relative flux error $\Delta F = \delta F / F$, where F is the flux value calculated over the averaging period $T = 30$ min. The relative flux error for N_2O flux is larger than the one estimated for sensible heat flux. For both fluxes the relative random uncertainty decreases with increasing flux magnitude. Moreover, in case of N_2O fluxes the relative errors are larger for negative flux values. This result indicates statistically less significant values in case of downward fluxes. Recently, Kroon et al. (2009) presented a detailed analysis of random and systematic uncertainty of N_2O flux measured by the EC technique. The random uncertainty, which accounted for 90% of their estimates of the total uncertainty, was calculated according to the error analysis introduced by Lumley and Panofsky (1964) and Wyngaard (1973),

$$\delta_\varphi = \sqrt{(2\tau_\varphi / T)}\sigma_\varphi \tag{3}$$

where T is the averaging period (e.g. 30 min), σ_ϕ and τ_ϕ are the standard deviation and the integral time scale of instantaneous flux $\phi = w'c'$. Error estimates given by Eq. (2) and Eq. (3) are two different methods to estimate the same flux random error, and their values are expected to be approximately the same (Rannik et al., 2009). A crucial point in using the Eq. (3) is to give a reasonable estimate of τ_ϕ, which can be numerically calculated from the autocorrelation function of the time series ϕ (Rannik et al., 2009). However, in practical applications of Eq. (3), τ_ϕ is often assumed to be approximately equal to z/U (Wyngaard, 1973; Pryor et al., 2008).

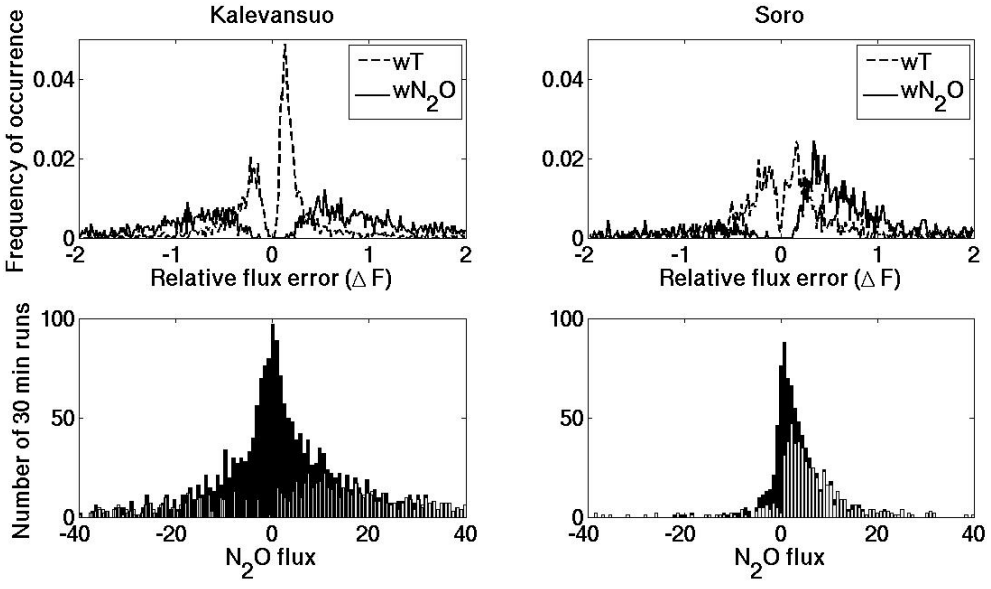

Fig. 7. In the top panels, the distribution curves of the relative flux error as estimated by $\delta F/F$ for sensible heat and N_2O fluxes for Kalevansuo and Sorø datasets. Bottom panels show the histograms of 30 min N_2O fluxes [$\mu g\,N\,m^{-2}\,h^{-1}$] prior (black bar) and after (grey bar) the random flux error criterion $\Delta F < 1$.

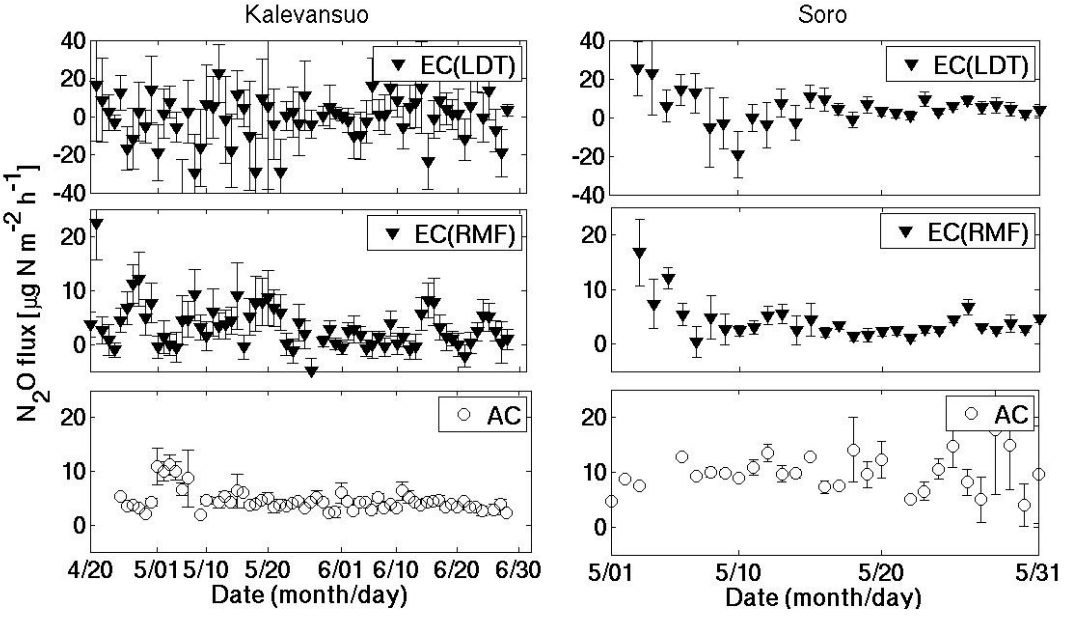

Fig. 8. Daily mean of N_2O fluxes measured by eddy covariance (top and middle panels) and automatic chambers (AC, bottom panels) during April–June 2007 at Kalevansuo pine forest and during May 2003 at Sorø beech forest. Eddy covariance fluxes are calculated by using linear detrending (EC-LDT) and running mean filter (EC-RMF). Error bars stand for standard error of the mean.

Although Kroon et al. (2009) used a different laser spectrometer (model QCL-TILDAS-76, Aerodyne Research Inc., USA), it is possible to compare the relative flux uncertainties estimated in this study and by Kroon et al. (2009), under the assumption that the main error sources are approximately the same. Since the relative flux error depends on flux magnitude, we select a flux range of 40–130 $\mu g\,N\,m^{-2}\,h^{-1}$ (the highest 30 min values measured at Kalevansuo), which corresponds to the low flux range of 15–35 $ng\,N\,m^{-2}\,s^{-1}$ reported by Kroon et al. (see their Table 3). For these flux values the average amount of relative random error, estimated for Kalevansuo, is about 76%, which is much smaller than the

Table 3. Mean and median fluxes of N_2O measured by eddy covariance (EC) and automatic chambers (AC) in Kalevansuo during 25 April–26 June 2007. All fluxes are in $\mu g\,N\,m^{-2}\,h^{-1}$.

Kalevansuo	Mean (stde)	Median (25th/75th perc)
N_2O_EC (LDT)	1.13 (1.38)	1.28 (−5.14/8.73)
N_2O_EC (RMF)	3.24 (0.5)	2.54 (0.2/5.1)
N_2O_EC ($\|\Delta F\| < 1$)	4.59 (0.96)	4.33 (0.32/7.1)
N_2O_AC	4.53 (0.03)	4.22 (3.28/5.04)

value of 308% measured by Kroon et al. (Note that this value refers to 90% of the total uncertainty reported in their Table 3). Such large difference of the estimated relative random errors is probably related to the parameterization that Kroon et al. (2009) used for the integral time scale in the Eq. (3), e.g. $\tau_\phi = 10z/U$, which differs by a factor of 10 with respect to that mentioned above. Accounting for the square root of this factor, the random uncertainty estimated by Kroon et al. (2009) would be 97%, which is of the same order of magnitude of the one we estimated in Kalevansuo. Then given the respective average flux magnitudes (18 and $25\,ng\,N\,m^{-2}\,s^{-1}$) in the selected range, the 30 min absolute uncertainty is $12\,ng\,N\,m^{-2}\,s^{-1}$ (equals $43\,\mu g\,N\,m^{-2}\,h^{-1}$) for Kalevansuo and $23\,ng\,N\,m^{-2}\,s^{-1}$ for Kroon et al. (2009) EC measurements.

In evaluation of average flux statistics, classification according to some threshold value of relative flux error is done. For example, by using $|\Delta F| < 1$, which means that for such subset the fluxes are with probability 68% within one standard deviation from the mean, as criterion to select the fluxes with higher confidence level (ie. with smaller random errors), the frequency distribution of N_2O flux values changes (less downward fluxes) as shown in the bottom panels of Fig. 7. However, we should acknowledge that the soil N_2O uptake seems not merely a result of random stochastic effect of flux values, as approximately 38% of 30 min downward fluxes for Kalevansuo and 12% for Sorø are statistically significant (larger than the estimated random flux error δF), which is in line with other studies reporting on occasional or even constant N_2O uptake in forest and agricultural ecosystems (e.g. Goossens et al., 2001; Butterbach-Bahl et al., 1998; Rosenkranz et al., 2006; Pihlatie et al., 2007; Chapuis-Lardy et al., 2007; Neftel et al., 2007). Thereby N_2O uptake often occurs under conditions of low nitrogen availability, which is especially true for the drained peatland forest site Kalevansuo (Pihlatie et al., 2009).

4.5 Comparison with chamber fluxes

For validation purpose, EC N_2O fluxes (corrected for high frequency loss) were compared to the soil N_2O flux rates simultaneously measured by automatic chambers during the field campaigns (see Pihlatie et al., 2005, 2009). Chambers were located 50 m northwest and 100 m southwest from the sub-canopy EC mast for Sorø and Kalevansuo site respectively.

Both of the measurement sites have limitations in a true method comparison between the EC and chamber fluxes. In Kalevansuo the automatic chambers were located slightly outside the estimated footprint area of the EC system (see Appendix B). However, as the vegetation and soil characteristics around both the automatic chambers and the sub-canopy EC mast was very similar, we can compare the fluxes obtained by these two methods. In Sorø, the automatic chamber was well within the footprint area of the EC system, however, as there was only one big automatic chamber, the comparison between the two methods is uncertain due to the high spatial variability in N_2O emissions at the measurement site (Pihlatie et al., 2005).

In order to smooth out the run-to-run variability and further reduce the flux random uncertainty, it is a common procedure to compare ensemble averaged flux statistics.

Comparison of daily mean values of EC and automatic chamber fluxes for Sorø and Kalevansuo are reported in Fig. 8. Top panels show EC fluxes calculated after applying a standard linear detrending operation to 30 min runs of N_2O and vertical wind velocity signals (EC-LDT). In middle panels a recursive high pass filter with a time constant equal to 50 s was applied prior flux calculation (EC-RMF). For Kalevansuo site EC-LDT fluxes are randomly distributed highly scattering around zero, which can mainly be related due to the N_2O signal drift. The Sorø EC-LDT fluxes show less scattering, but unexpected high N_2O uptake rates ($> 10\,\mu g\,N\,m^{-2}\,h^{-1}$) for some days. The randomly large scattering are significantly reduced in EC-RMF fluxes (especially in Kalevansuo), which are comparable with the magnitude of chamber fluxes at both sites. A comprehensive analysis of temporal variability of N_2O emission and environmental driving factors is reported in Pihlatie et al. (2005) for Sorø and Pihlatie et al. (2009) for Kalevansuo site.

Mean and median values of EC fluxes calculated over the entire campaign periods with different methods (LDT or RMF) and selected according to confidence level criteria (ΔF) are compared with the automatic chambers flux statistics (Tables 3 and 4). In most of the cases the mean and median values of EC fluxes were smaller than the corresponding values by the automatic chamber (AC) technique, however showing a larger statistical uncertainty and dispersion as indicated by the mean standard error (stde) and the 25th/75th percentile values respectively. The EC flux statistics from the distribution of 30 min flux calculated by LDT method show the largest departure from the AC flux statistics. For

Table 4. Mean and median fluxes of N_2O measured by eddy covariance (EC) and automatic chambers (AC) in Sorø during 3 May–31 May 2003. All fluxes are in $\mu g\,N\,m^{-2}\,h^{-1}$.

Sorø	Mean (stde)	Median (25th/75th perc)
N_2O_EC (LDT)	4.01 (0.3)	3.44 (1.1/7.2)
N_2O_EC (RMF)	4.79 (0.7)	3.61 (2.5/5.1)
N_2O_EC ($\|\Delta F\| < 1$)	7.2 (0.4)	5.33 (3.8/8.0)
N_2O_AC	9.85 (0.12)	9.6 (7.55/12.53)

Kalevansuo dataset the LDT based estimate of N_2O emission in $\mu g\,N\,m^{-2}\,h^{-1}$ was 1.13 (stde=1.38) as mean value and 1.28 (25th/75th percentiles = $-5.14/8.73$) as median value, while the corresponding statistics for Sorø were 4.01 (stde=1.2) and 3.44 (25th/75th=1.1/7.2). The weak significance of LDT flux statistics is due to randomly large values frequently observed (especially for Kalevansuo) during periods characterized by low frequency variability in N_2O concentrations, mainly due to the instrumental drift. The RMF method reduces the scatter and variability of the fluxes, and at the same time producing an increase of the estimated average N_2O emission, which is notable in Kalevansuo and relatively small in Sorø dataset. Again this suggests stronger effects of optical interference fringes during the Kalevansuo campaign.

For further validation and comparison purpose, the measured 30 min fluxes were conditionally selected according to the estimated values of ΔF. Here we used a threshold, $|\Delta F| < 1$, noting that for a Gaussian distribution 68% of data values is within $\pm 1\sigma$ of the mean. Despite the fact that 30 min downward N_2O fluxes are only partly removed by such criterion (Sect. 4.4), at both sites ensemble EC flux statistics get closer to the whole period net flux values estimated by automatic chamber technique (Tables 3 and 4).

5 Conclusions

EC measurements of N_2O fluxes with today's commercially available trace gas analyzers for N_2O are still a challenge, and careful consideration of instrument performance is needed. Moreover, for this case study, the special condition of turbulent trace gas measurements in the forest trunk space requires an in-depth assessment and evaluation of the data obtained. Therefore, the focus of this paper was on quality control aspects related to data processing as well as an error analysis related to flux sampling. With respect to data processing, our results highlight that fringe effects in the N_2O signal, measured by TDL spectrometers (TGA100 and TGA100A, Campbell Scientific Inc.), can have a strong impact on the quality of the N_2O EC flux values. Although an active thermal control of the TDL enclosure in theory could help to partially eliminate this effect (Billesbach et al., 1998), further tests in the field are needed to assess the efficiency. On the other hand, this case study has demonstrated that signal processing strategies are still a key issue to assure the quality of trace gas flux measurements based upon such complex systems (Werle et al., 2004). In this context, the concept of the Allan variance is a valuable tool to characterize system stability and in the time domain it provides similar information as spectral analysis in the frequency domain. It was found that during post sampling data processing a high-pass filter time constant of 50 s was able to reduce the fringe effect. The LDT method and RMF method with time constant > 100 s (not shown here) lead to increased scatter in fluxes during periods characterized by low frequency variability in concentrations, mainly due to instrument drift.

Flux error analysis, traditionally used in the micrometeorological community for energy and CO_2 fluxes, has been applied to N_2O flux measurements, in order to identify uncertainty of fluxes caused by instrumentation problems and systematic as well as random errors. Although for our EC measurement systems systematic errors due to low pass filter effects of measured fluxes were rather small, we demonstrated that the cospectral transfer function method is a suitable approach for correcting fluxes measured within canopy layer. EC N_2O flux measurements showed larger random uncertainty than the other measured EC fluxes, and classification according to statistical significance of single flux values indicates that downward N_2O fluxes are associated with larger random errors. Finally we demonstrated that the estimated RMF fluxes show less scatter and random variability compared to LDT based fluxes, and they are in better agreement with the N_2O fluxes resulting from automatic soil chamber measurements.

Appendix A

Allan variance analysis

The Allan variance plot is a graphical data analysis technique for examining the low-frequency component of a time series. Generally this technique is applied with lab calibration gas in order to assess the system precision and stability, which obviously will depend on the drift of the instrument (Werle, 2009). For an illustrative purpose, let's to consider a simulated data time-series $X_i, i = 1,\ldots,$N with N=2^q (q is a positive integer), represented by $X = a + bt$+WN, where $a = 320$ is the offset, $b = 2$ is a linear drift coefficient, $t = i/$N and WN is a white noise (Gaussian) distribution with zero mean and variance equal to 0.1 (top panel of Fig. A1). The Allan variance for each "scale" $k = 1,\ldots,$ N/2 is defined as:

$$\sigma_a^2(k) = \frac{1}{2(\mathrm{m}-1)} \sum_{s=1}^{\mathrm{m}-1} \left[A_{s+1}(k) - A_s(k)\right]^2 \qquad \text{(A1)}$$

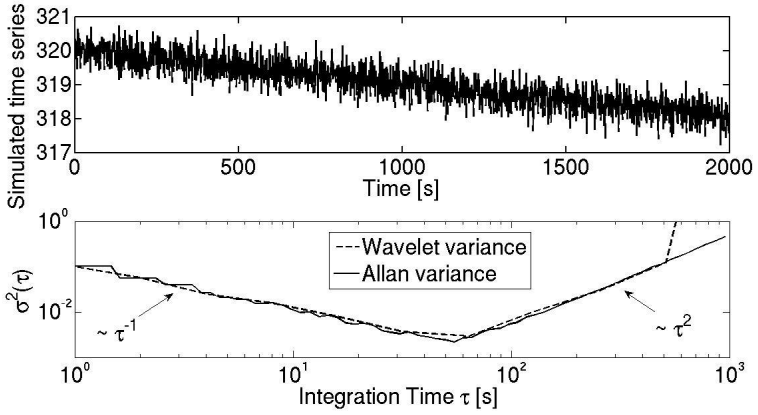

Fig. A1. Top panel: Simulated time series data containing white noise and a linear negative drift. Bottom panel: Allan plots of the simulated data, computed by Eq. A1 (solid line) and by Eq. A3 (dashed line).

where $m = N/k$ is the number of subsamples and A_s is the time-average of the signal X over subsample period s of size k, given by

$$A_s(k) = \frac{1}{k}\sum_{p=1}^{k} X_{(sk+p)} \tag{A2}$$

Assuming that the time series data is sampled at constant sampling frequency f_s, then the time $\tau = k/f_s$ is the integration time or the averaging time of subsample periods under the assumption that no dead time losses due to signal processing occurs (Werle et al., 1993).

According to Percival and Guttorp (1994), the Allan variance at scale k is directly related to the variance of the Haar wavelet coefficients at the same scale. Then an alternative estimator for the Allan variance is

$$\hat{\sigma}_a^2(k) \equiv \frac{2}{N}\sum_{j=1}^{N/2k} d_{j,k}^2 \tag{A3}$$

Where $d_{j,k}$ are the wavelet coefficients for scales $k = 1, 2, 4, \ldots$,N/2, derived applying the Haar wavelet transform to the time series X (Percival and Guttorp, 1994).

The bottom panel of Fig. A1 shows the Allan variance curves of the simulated time series X, estimated by using Eq. (A1) and Eq. (A3) as a function of the integration time τ.

The Allan variance decreases as τ^{-1} when white noise dominates. At longer integration times, the Allan variance starts to increase, due to the signal drift. If a linear drift dominates, then the increase of the Allan variance obeys to τ^2 law.

Appendix B

Footprint analysis

Footprint analysis for the Sorø site was already published by Pihlatie et al. (2005) and it is not repeated in this study. According to Pihlatie et al. (2005), the area contributing 85% to the EC flux lies within 60 m ($x/h_c = 2.4$) around the measurement mast.

At Kalevansuo site footprint functions for passive tracers released from the forest floor were calculated with the forward Lagrangian stochastic model as described by Rannik et al. (2000, 2003). The model predicted the horizontal distribution of the surface sources of the flux measurements for three selected wind direction (WD) sectors ($140° < \mathrm{WD} < 190°$, $190° < \mathrm{WD} < 240°$ and $240° < \mathrm{WD} < 320°$) and for two stability classes (near-neutral and unstable conditions, defined for values of $|L| > 200$ and $-200 < L < 0$ respectively, where L is the Obukhov length measured above canopy). As fluxes and characteristics of turbulence were measured only at two heights – one within the canopy and one above – the forms of the profiles of flow statistics were adopted from the work by Rannik et al. (2003). However, to account for the actual flow characteristics the profiles were scaled to go through the present observations.

Estimated footprint functions were rather similar for different wind direction sectors and they show a rather small influence of stability conditions at the sub-canopy reference height $z/h_c = 0.25$. The upwind distance x corresponding to 85% of cumulative footprint values was about 30 m ($x/h_c = 1.87$).

Acknowledgements. The study was supported by EU projects Nitroeurope-IP, IMECC, ICOS and Academy of Finland.

Edited by: H. Lankreijer

References

Ambus, P. and Christensen, S.: Spatial and seasonal nitrous oxide and methane fluxes in Danish forest-, grassland-, and agroecosystems, J. Environ. Qual., 24, 993–1001, 1995.

Amiro, B. D.: Drag coefficients and turbulence spectra within three boreal forest canopies, Bound.-Lay. Meteorol., 52, 227–246, 1990.

Aubinet, M., Grelle, A., Ibrom, A., Rannik, Ü., Moncrieff, J., Foken, T., Kowalski, A. S., Martin, P. H., Berbigier, P., Bernhofer, C., Clement, R., Elbers, J., Granier, A., Grünvald, T., Morgenstern, K., Pilegaard, K., Rebmann, C., Snijders, W., Valentini, R., and Vesala, T.: Estimates of the annual net carbon and water exchange of European forests: the EUROFLUX methodology, Adv. Ecol. Res., 30, 113–175, 2000.

Billesbach, D. P., Kim, J., Clement, R. J., Verma, S. B., Ullman, F. G.: An intercomparison of two tunable diode laser spectrometers used for eddy correlation measurements of methane flux in a prairie wetland, J. Atmos. Ocean. Tech., 15, 197–206, 1998.

Brodeur, J. J., Warland, J. S., Staebler, R. M., and Wagner-Riddle, C.: Technical note: Laboratory evaluation of a tunable diode laser system for eddy covariance measurements of ammonia flux, Agr. Forest Meteorol., 149, 385–391, 2009.

Butterbach-Bahl, K., Gasche, R., Huber, C. H., Kreutzer, K. and Papen, H.: Impact of N-input by wet deposition on N-trace gas fluxes and CH_4 oxidation in spruce forest ecosystems of the temperate zone in Europe, Atmos. Environ., 32, 559–564, 1998.

Campbell Scientific Inc: TGA100 trace gas analyzer user and reference manual, Campbell Scientific Inc, 2004.

Cava, D., Giostra, U., Siqueira, M. B. B., and Katul, G. G.: Organised motion and radiative perturbations in the nocturnal canopy sublayer above an even-aged pine forest, Bound.-Lay. Meteorol., 112, 129–157, 2004.

Chapuis-Lardy, L., Wrage, N., Metay, A., Chotte, J.-L. and Bernoux, M.: Soils, a sink for N_2O? A review, Glob. Change Biol., 13, 1–17, doi:10.1111/j.1365-2486.2006.01280.x, 2007.

Christensen, S., Ambus, P., Arah, J. R., Clayton, H., Galle, B., Griffith, D. W. T., Hargreaves, K. J., Klemedtsson, L., Lind, A. M., Maag, M., Scott, A., Skiba, U., Smith, K. A., Welling, M., and Wienhold, F. G.: Nitrous oxide emissions from an agricultural field: comparison between measurements by flux chamber and micrometeorological techniques, Atmos. Environ., 30(24), 4183–4190, 1996.

Eugster, W. and Senn, W.: A cospectral correction model for measurement of turbulent NO_2 flux, Bound.-Lay. Meteorol., 74, 321–340, 1995.

Eugster, W., Zeyer, K., Zeeman, M., Michna, P., Zingg, A., Buchmann, N., and Emmenegger, L.: Methodical study of nitrous oxide eddy covariance measurements using quantum cascade laser spectrometery over a Swiss forest, Biogeosciences, 4, 927–939, 2007,
http://www.biogeosciences.net/4/927/2007/.

Flechard, C., Neftel, A., Jocher, M., Amman, C.: Bi-directional soil-atmosphere N_2O exchange over two mown grassland systems with contrasting management practices, Glob. Change Biol., 11, 2114–2127, 2005.

Goossens, A., De Visscher, A., Boeckx, P., and Van Cleemput, O.: Two-year field study on the emission of N_2O from coarse and middle textured Belgian soils with different land use, Nutr. Cycl. Agroecos., 60, 23–34, 2001.

Hernandez, G.: Fabry-Perot interferometers, Cambridge Publishing, 343 pp., 1986.

Horst, T. W.: A simple formula for attenuation of eddy fluxes measured with first-order-response scalar sensors, Bound.-Lay. Meteorol., 82, 219–233, 1997.

IPCC: Climate change 2001, The Scientific Basis, Cambridge University Press, Cambridge, UK, 2001.

Kaimal, J. C. and Finnigan, J. J.: Atmospheric Boundary Layer Flows, Their Structure and Measurement, Oxford University Press, New York, 1994.

Kaimal, J. C., Wyngaard, J. C., Izumi, Y., Cote, O. R.: Spectral characteristics of surface-layer turbulence, Quart. J. Roy. Meteorol. Soc., 98, 563–589, 1972.

Katul, G. G., Geron, C. D., Hsieh, C.-I., Vidakovic, B., Guenther, A. B., Active turbulence and scalar transport near the forest-atmosphere interface, J. Appl. Meteorol., 37, 1533–1546, 1998.

Kesik, M., Ambus, P., Baritz, R., Brggemann, N., Butterbach-Bahl, K., Damm, M., Duyzer, J., Horváth, L., Kiese, R., Kitzler, B., Leip, A., Li, C., Pihlatie, M., Pilegaard, K., Seufert, G., Simpson, D., Skiba, U., Smiatek, G., Vesala, T., and Zechmeister-Boltenstern, S.: Inventories of N_2O and NO emissions from European forest soils, Biogeosciences Discuss., 2, 779–827, 2005,
http://www.biogeosciences-discuss.net/2/779/2005/.

Kormann, R., Mueller, H., and Werle, P.: Eddy flux measurements of methane over the fen Murnauer Moos, 11°11′ E, 47°39′ N, using a Fast Tunable Diode-Laser Spectrometer, Atmos. Environ., 35, 2533–2544, 2001.

Kroon, P. S., Hensen, A., Jonker, H. J. J., Zahniser, M. S., van 't Veen, W. H., and Vermeulen, A. T.: Suitability of quantum cascade laser spectroscopy for CH_4 and N_2O eddy covariance flux measurements, Biogeosciences, 4, 715–728, 2007,
http://www.biogeosciences.net/4/715/2007/.

Kroon, P. S., Hensen, A., Jonker, H. J. J., Ouwersloot, H. G., Vermeulen, A. T., and Bosveld F. C.: Uncertainties in eddy covariance flux measurements assessed from CH_4 and N_2O observations, Agr. Forest Meteorol., in press, doi:10.1016/j.agrformet.2009.08.008, 2009.

Laville, P., Henault, C., Renault, P., Cellier, P., Oriol, A., Devis, X., Flura, D., and Germon, J. C.: Field comparison of nitrous oxide emission measurements using micrometeorological and chamber methods, Agronomie, 17, 375–388, 1997.

Lee, X. L., Massman, W., and Law, B.: Handbook of micrometeorology, Kluwer Academic Publisher, Dordrecht, The Netherlands, 2004.

Lenschow, D. H., Mann, J., and Christens, L.: How long is long enough when measuring fluxes and other turbulence statistics? , J. Atmos. Ocean. Tech., 11, 661–673, 1994.

Lumley, J. L. and Panofsky, H. A.: The structure of atmospheric turbulence, Wiley and Sons, 239 pp., 1964.

Mammarella, I., Launiainen, S., Gronholm, T., Keronen, P., Pumpanen, J., Rannik, Ü., and Vesala, T.: Relative humidity effect on the high frequency attenuation of water vapour flux measured by a closed-path eddy covariance system, J. Atmos. Ocean. Tech., 26(9), 1856–1866, 2009.

McMillen, R. T.: An eddy correlation technique with extended applicability to non-simple terrain, Bound.-Lay. Meteorol., 43, 231–245, 1988.

Moncrieff, J. B., Massheder, J. M., de Bruin, H., Elbers, J., Friborg, T., Heusinkveld, B., Kabat, P., Scott, S., Soegaard, H., and

Verhoef, A.: A system to measure surface fluxes of momentum, sensible heat, water vapour and carbon dioxide, J. Hydrol., 188–189, 589–611, 1997.

Moore, C. J.: Frequency response corrections for eddy correlation systems, Bound.-Lay. Meteorol., 37, 17–35, 1986.

Neftel, A., Flechard, C., Ammann, C., Conen, F., Emmenegger, L. and Zeyer, K.: Experimental assessment of N_2O background fluxes in grassland systems, Tellus B, 59, 470–482, 2007.

Neftel, A., Ammann, C., Fischer, C., Spirig, C., Conen, F., Emmenegger, L., Tuzson, B., Wahlen, S.: N_2O exchange over managed grassland: Application of a quantum cascade laser spectrometer for micrometeorological flux measurements, Agr. Forest Meteorol., in press, doi:10.1016/j.agrformet.2009.07.013, 2009.

Nelson, D. D., Shorter, J. H., McManus, J. B., and Zahniser, M. S.: Sub-part-per-billion detection of nitric oxide in air using a thermoelectrically cooled mid-infrared quantum cascade laser spectrometer, Appl. Phys. B, 75, 343–350, 2002.

Percival, D. B. and Guttorp, P.: Long-memory processes, the Allan variance and wavelets, edited by: Foufoula-Georgiou, E. and Kumar, P., Wavelets in Geophysics, Academic Press, US, 325–344, 1994.

Pihlatie, M., Rinne, J., Ambus, P., Pilegaard, K., Dorsey, J. R., Rannik, Ü., Markkanen, T., Launiainen, S., and Vesala, T.: Nitrous oxide emissions from a beech forest floor measured by eddy covariance and soil enclosure techniques, Biogeosciences, 2, 377–387, 2005

Pihlatie, M. K., Kiese, R., Brüggemann, N., Butterbach-Bahl, K., Kieloaho, A.-J., Laurila, T., Lohila, A., Mammarella, I., Minkkinen, K., Penttilä, T., Schönborn, J., and Vesala, T.: Greenhouse gas fluxes in a drained peatland forest during spring frost-thaw event, Biogeosciences Discuss., 6, 6111–6145, 2009, http://www.biogeosciences-discuss.net/6/6111/2009/.

Rannik, Ü. and Vesala, T.: Autoregressive filtering versus linear detrending in estimation of fluxes by the eddy covariance method, Bound.-Lay. Meteorol., 91, 259–280, 1999.

Rannik, Ü., Aubinet, M., Kurbanmuradov, O., Sabelfeld, K. K, Markkanen, T., and Vesala, T.: Footprint analysis for measurements over a heterogeneous forest, Bound.-Lay. Meteorol., 97, 137–166, 2000.

Rannik, Ü., Markkanen, T., Raittila, J., Hari, P., and Vesala, T.: Turbulence statistics inside and over forest: Influence on footprint prediction, Bound.-Lay. Meteorol., 109, 163–189, 2003.

Rannik, Ü., Mammarella, I., Aalto, P., Keronen, P., Vesala, T., and Kulmala, M.: Long-term aerosol particle flux observations Part I: Uncertainties and time-averaged statistics, Atmos. Environ., 43(21), 3431–3439, 2009.

Rosenkranz, P., Brüggemann, N., Papen, H., Xu, Z., Seufert, G., and Butterbach-Bahl, K.: N_2O, NO and CH_4 exchange, and microbial N turnover over a Mediterranean pine forest soil, Biogeosciences Discuss., 2, 673–702, 2005, http://www.biogeosciences-discuss.net/2/673/2005/.

Scanlon, T. M. and Kiely, G.: Ecosystem-scale measurements of nitrous oxide fluxes for an intensely grazed, fertilized grassland, Geophys. Res. Lett., 30(16), 1852, doi:10.1029/2003GL017454, 2003.

Silver, W. L., Thompson, A. W., McGroddy, M. E., Varner, R. K., Dias, J. D., Silva, H., Crill, P., and Kellers, M.: Fine root dynamics and trace gas fluxes in two lowland tropical forest soils, Glob. Change Biol., 11, 290–306, 2005.

Skiba, U., Fowler, D., and Smith, K. A.: Emissions of NO and N_2O from soils, Environ. Mon. Assess., 31, 153–158, 1994.

Smith, K. A., Clayton, H., Arah, J. R. M., Christensen, S., Ambus, P., Fowler, D., Hargreaves, K. J., Skiba, U., Harris, G. W., Wienhold, F. G., Klemedtsson, L., and Galle, B.: Micrometeorological and chamber methods for measurement of nitrous oxide fluxes between soils and the atmosphere: Overview and conclusions, J. Geophys. Res., 99(D8), 16541–16548, 1994.

Vickers, D. and Mahrt, L.: Quality control and flux sampling problems for tower and aircraft data, J. Atmos. Ocean. Tech., 14, 512–526, 1997.

Webb, E. K., Pearman, G. I., and Leuning, R.: Correction of flux measurements for density effects due to heat and water vapour transfer, Quart. J. Roy. Meteor. Soc., 106, 85–100, 1980.

Werle, P., Muecke, R., and Slemr, F.: The limits of signal averaging in atmospheric trace gas monitoring by tunable diode-laser absorption spectroscopy, Appl. Phys. B, 57, 131–139, 1993.

Werle, P., Mazzinghi, P., D'Amato, F., De Rosa, M., Maurer, K., Slemr, F.: Signal processing and calibration procedures for in-situ diode-laser absorption spectroscopy, Spectrochim. Acta A, 60, 1685–1705, 2004.

Werle, P.: Time domain characterization of micrometeorological data based on a two sample variance, Agr. Forest Meteorol., in press, doi:10.1016/j.agrformet.2009.12.007, 2009.

Wienhold, F. G., Frahm, H., and Harris, G. W.: Measurements of N_2O fluxes from fertilized grassland using a fast response tunable diode laser spectrometer, J. Geophys. Res., 99(D8), 16557–16567, 1994.

Wyngaard, J. C.: On the surface layer turbulence, edited by: Haugen, D. A., Workshop on micrometeorology, Boston, AMS, 101–149, 1973.